Supporting Information

Stirring Revealed New Functions of Ethylenediamine and Hydrazine in the Morphology Control of Copper Nanowires

Juan Zhang,[a] Xiaona Li,[a] Dongmei Liu,[a] Shuai Wang,[a] Jiaxu Yan,[a] Min Lu,*[a] Xiaoji Xie,*[a] Ling Huang[a] and Wei Huang[a,b]

[a]*Key Laboratory of Flexible Electronics (KLOFE), Institute of Advanced Materials (IAM), Nanjing Tech University (NanjingTech), Nanjing 211816, China*

[b]*Shaanxi Institute of Flexible Electronics (SIFE), Northwestern Polytechnical University, 127 West Youyi Road, Xi'an 710072, China.*

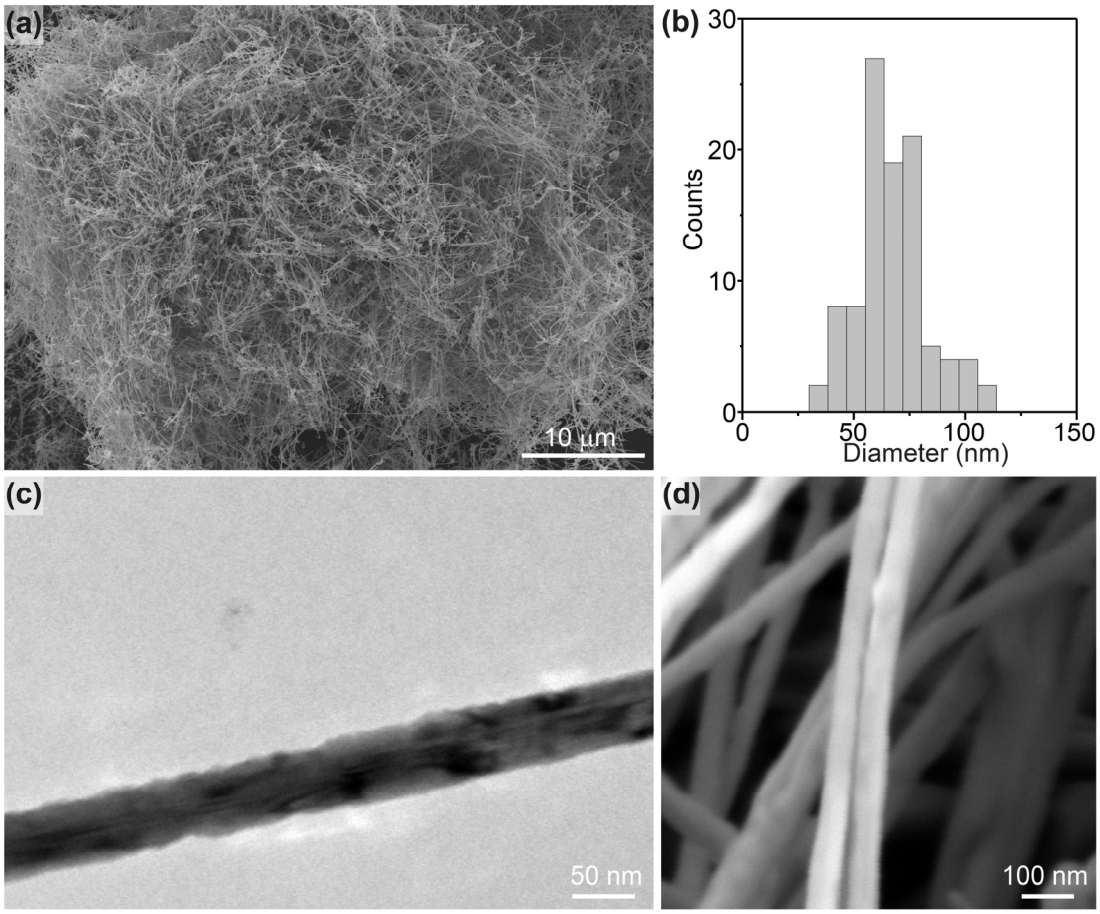

Fig. S1 (a) Large scale SEM image of the obtained smooth Cu nanowires and (b) corresponding diameter distribution. (c) Enlarged TEM image of a smooth Cu nanowire. (d) Enlarged SEM image of smooth Cu nanowires.

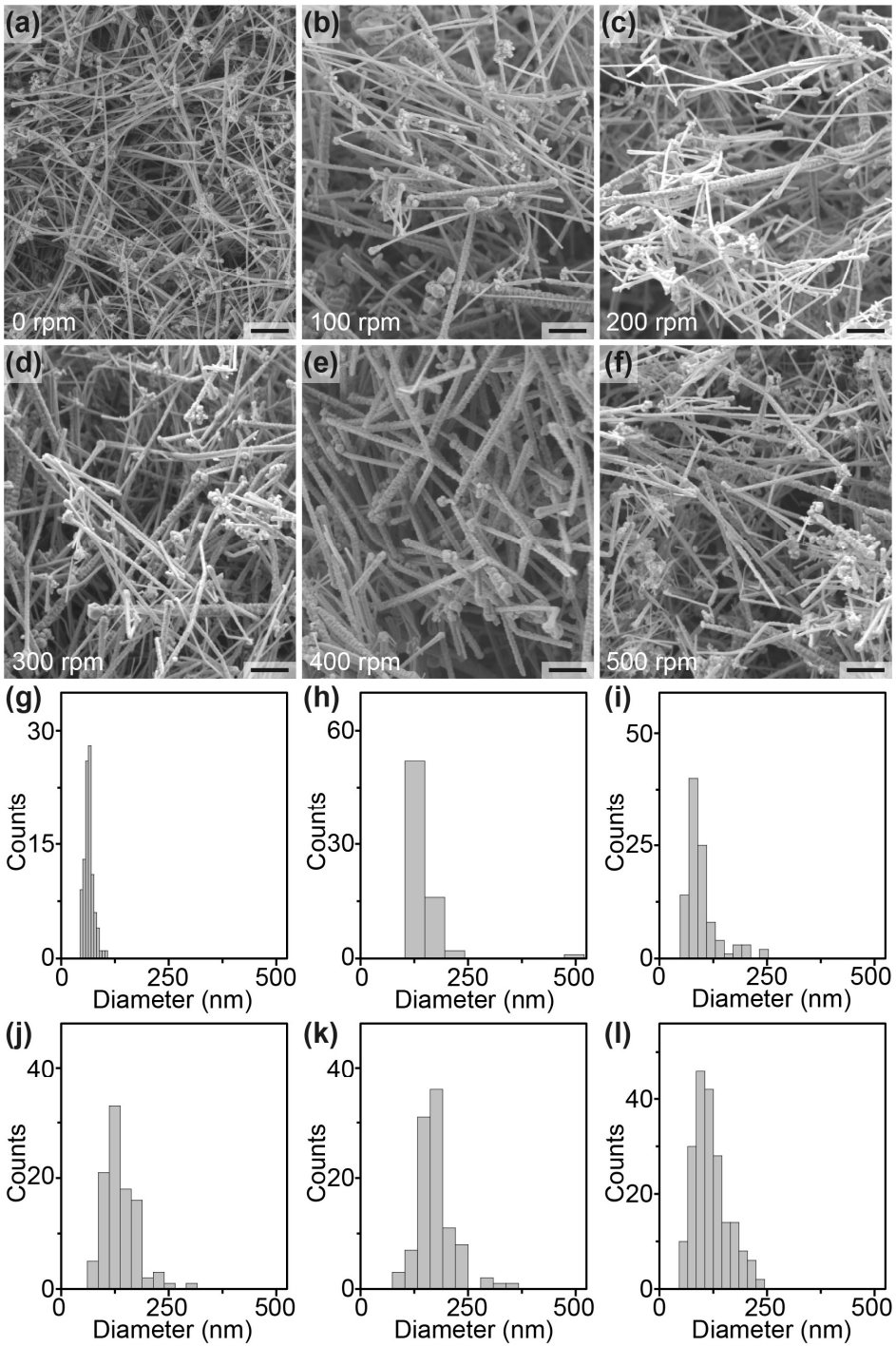

Fig. S2 (a-f) SEM images of Cu nanowires prepared with the addition of 100 μL EDA and 30 μL N_2H_4 under different stirring rates, and (g-l) corresponding diameter distributions. The stirring rates for (a-l) are (a, g) 0, (b, h) 100, (c, i) 200, (d, j) 300, (e, k) 400 and (f, l) 500 rpm, respectively. The scale bars are 1 μm for (a-f).

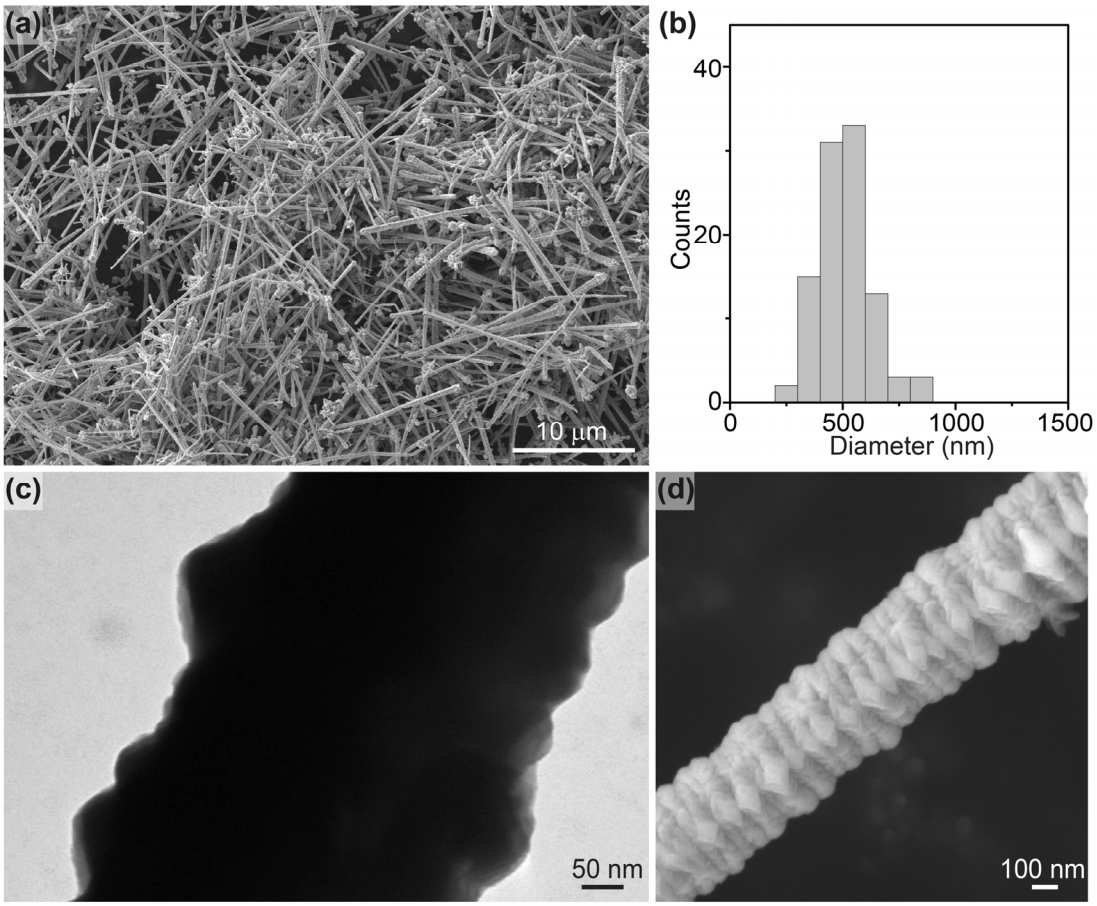

Fig. S3 (a) Large scale SEM image of the obtained rough Cu nanowires and (b) corresponding diameter distribution. Note that the diameter of rough Cu nanowires is measured near the big-sized head. (c) Enlarged TEM image of a rough Cu nanowire. (d) Enlarged SEM image of a rough Cu nanowire.

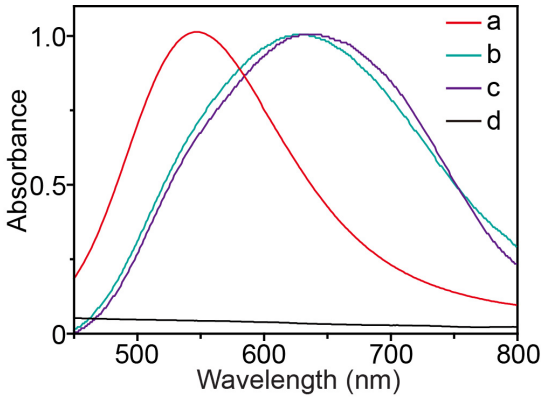

Fig. S4 UV-vis absorption spectra of (a) the mixture of $Cu(NO_3)_2$ and EDA, (b) the mixture of NaOH and $Cu(NO_3)_2$, (c) the mixture of NaOH, $Cu(NO_3)_2$, and EDA, and (d) the mixture of NaOH, $Cu(NO_3)_2$, EDA, and N_2H_4, respectively. Note that the spectra of (a, b, and c) are normalized for comparison.

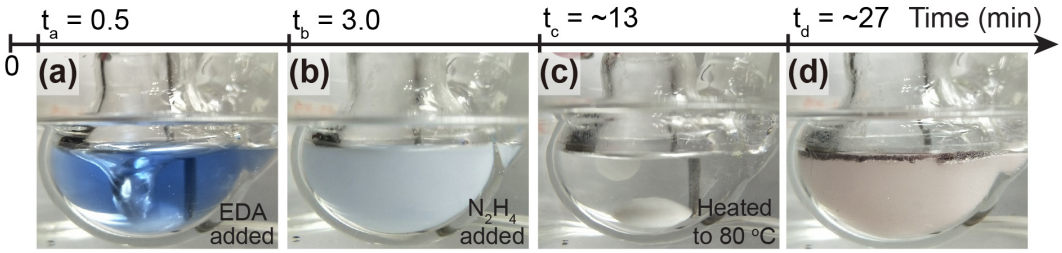

Fig. S5 Recorded synthetic process of rough Cu nanowires. (a-d): photos of the reaction mixture (a) after the addition of EDA, (b) 2 minutes after the addition of N_2H_4, (c) after heated to 80 °C, and (d) with rough Cu nanowire products, respectively. Note that the timeline on top illustrates the progress of the reaction, and the beginning of the reaction (t = 0 min) is denoted as the time point when $Cu(NO_3)_2$ is added to the reaction system.

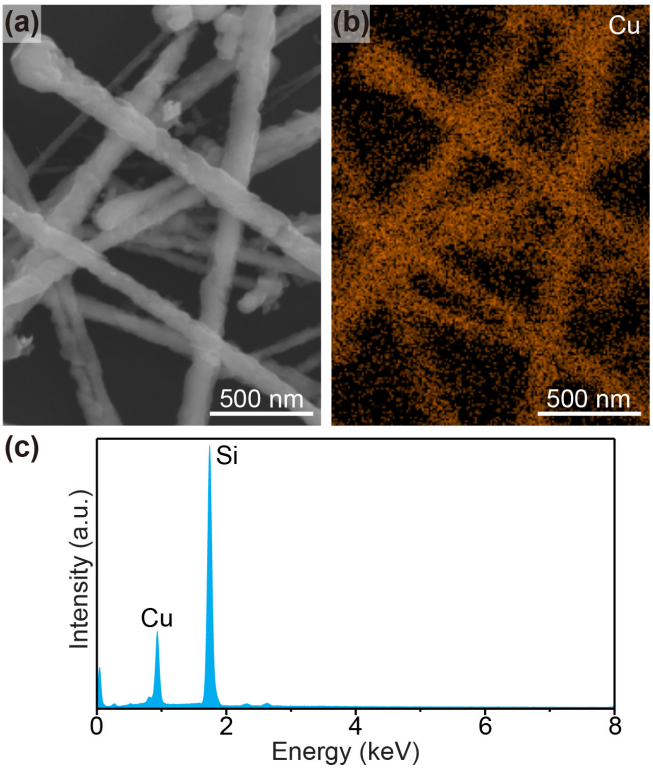

Fig. S6 (a) SEM image, (b) corresponding elemental mapping and (c) corresponding EDX spectrum of products extracted from the reaction mixture, during the synthesis of smooth Cu nanowires, after the reaction continues for ~17 minutes. The corresponding large scale SEM image is shown in Fig. 2b3. The EDX analysis indicates that the products are Cu nanowires after the reaction continues for ~17 minutes. The signal of Si element is due to the use of Si substrate for sample fixing.

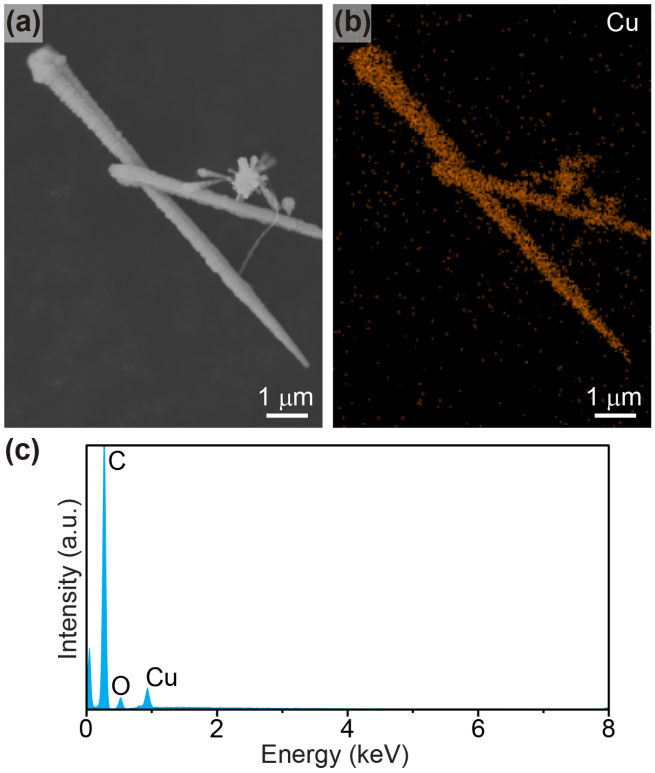

Fig. S7 (a) SEM image, (b) corresponding elemental mapping and (c) corresponding EDX spectrum of products extracted from the reaction mixture, during the synthesis of rough Cu nanowires, after the reaction continues for ~27 minutes. The corresponding large scale SEM image is shown in Fig. 2c3. The EDX analysis indicates that the products are Cu nanowires after the reaction continues for ~27 minutes. The signal of C and O elements should be due to the use of conductive carbon tapes for sample fixing.

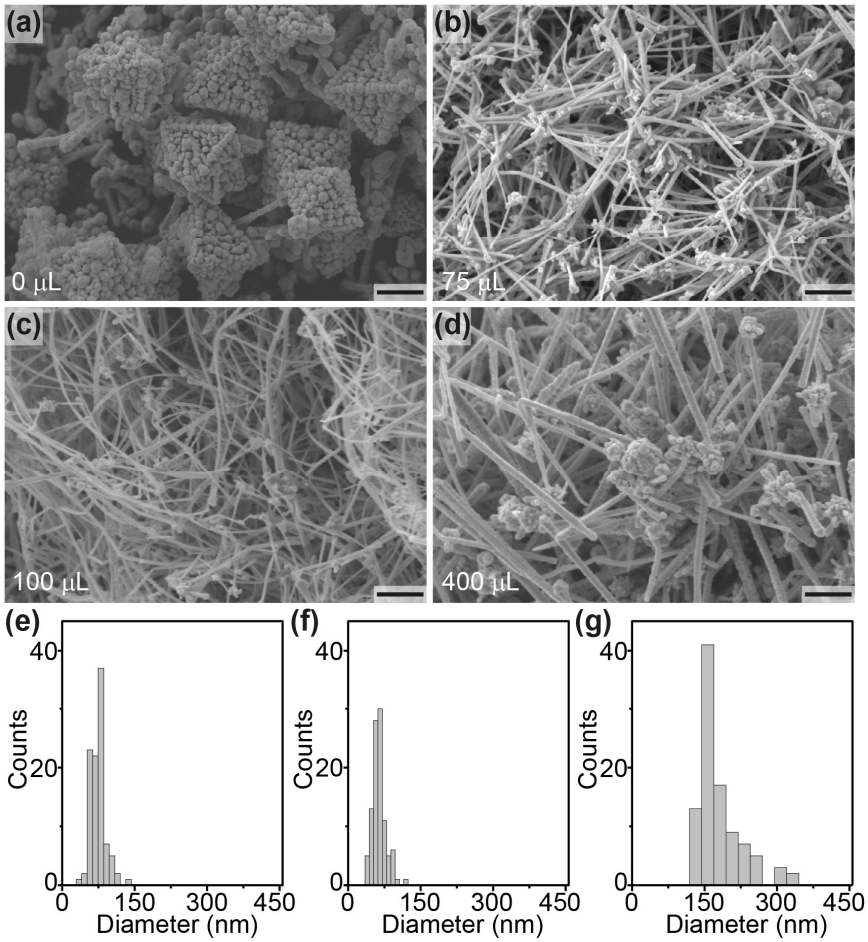

Fig. S8 (a-d) SEM images of products synthesized with the addition of different amounts of EDA. (a-d): 0, 75, 100, and 400 μL of EDA, respectively. Note that other reaction conditions are identical to those for synthesizing smooth Cu nanowires, and the scale bars are 1 μm for (a-d). (e-g) Corresponding diameter distributions of Cu nanowires shown in (b-d), respectively.

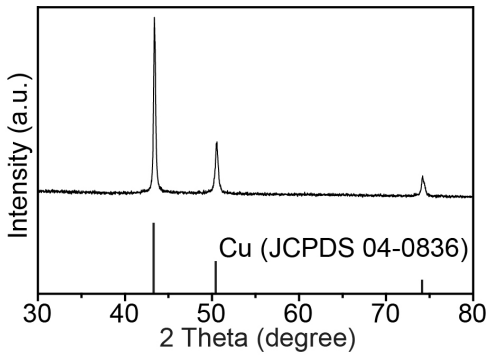

Fig. S9 Corresponding XRD pattern of the products shown in Fig. S8a. The diffraction pattern at the bottom is the literature reference for cubic Cu crystals (JCPDS 04-0836).

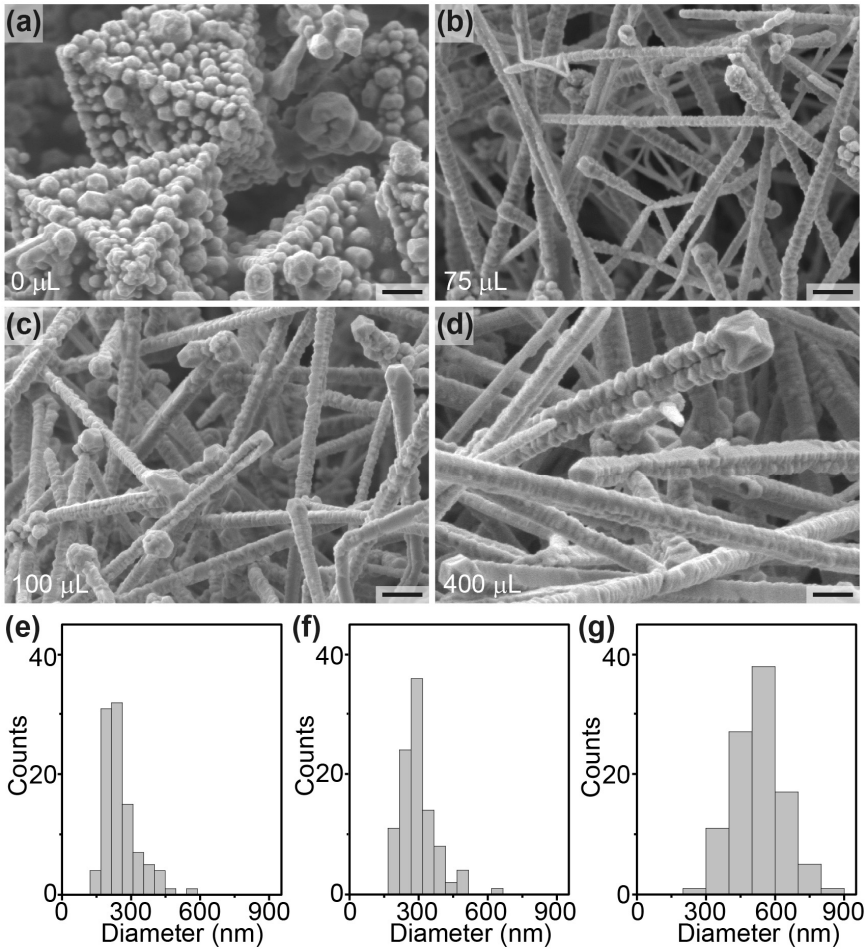

Fig. S10 (a-d) SEM images of products synthesized with the addition of different amounts of EDA under steady stirring (200 rpm). (a-d): 0, 75, 100, and 400 μL of EDA, respectively. Note that other reaction conditions are identical to those for synthesizing rough Cu nanowires, and the scale bars are 500 nm for (a-d). (e-g) Corresponding diameter distributions of Cu nanowires shown in (b-d), respectively. The diameters of rough Cu nanowires are measured near the big-sized head.

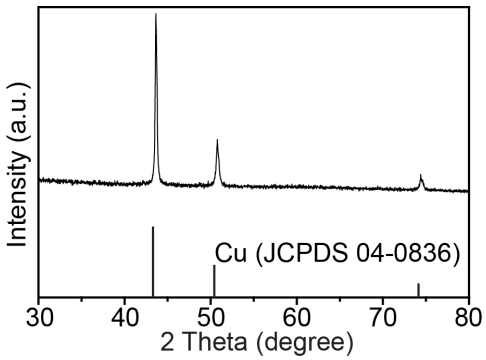

Fig. S11 Corresponding XRD pattern of the products shown in Fig. S10a. The diffraction pattern at the bottom is the literature reference for cubic Cu crystals (JCPDS 04-0836).

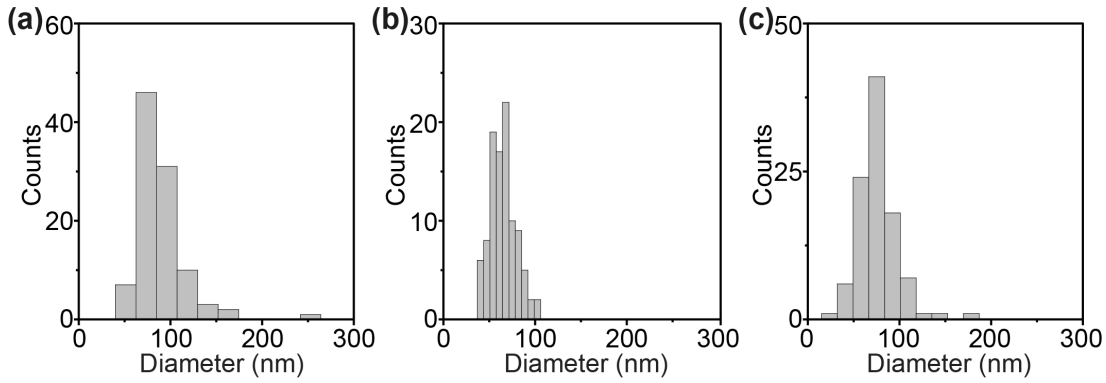

Fig. S12 (a-c) Corresponding diameter distributions of Cu nanowires shown in Fig. 3a-c, respectively.

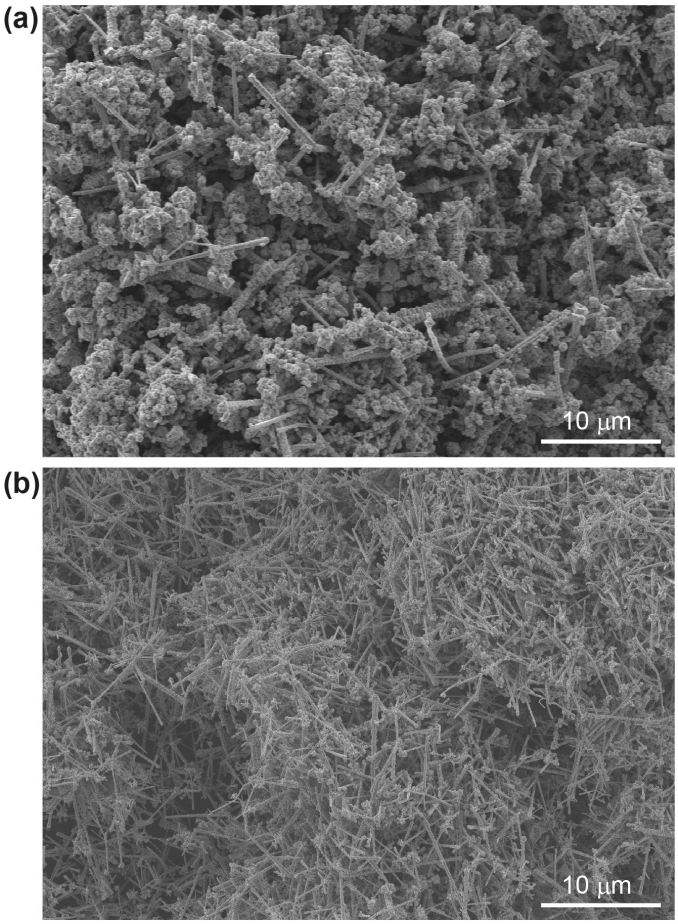

Fig. S13 Large scale SEM images of products synthesized under different stirring rates (a: 200 rpm, b: 400 rpm) by using 40 μL of N_2H_4. Note that other reaction conditions are identical to those for synthesizing rough Cu nanowires.

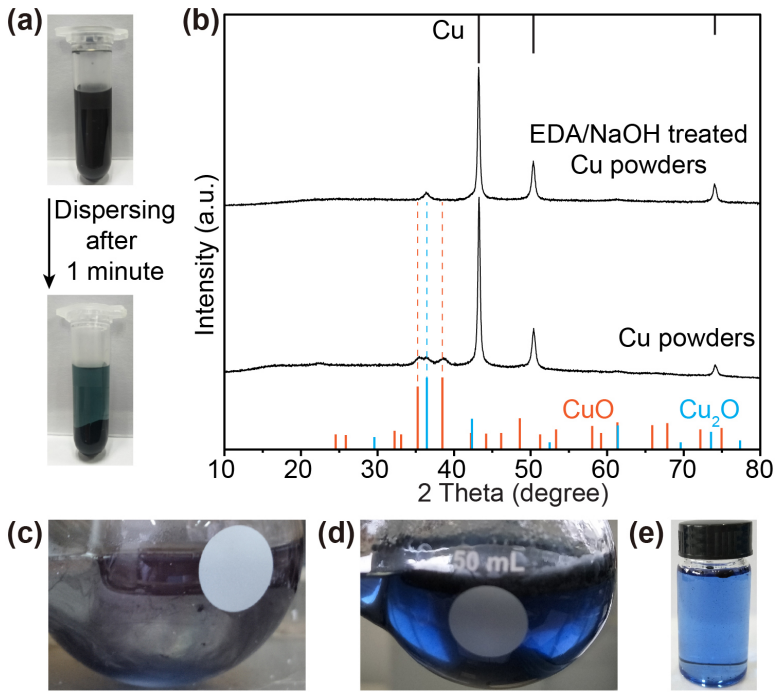

Fig. S14 (a) Photos of the tube containing a mixture of Cu powders (45 mg), and EDA (1.5 mL). The Cu powders were dispersed in EDA by sonication for 1 minute. Note that the color change of the supernatant indicates a reaction between Cu powders and EDA. (b) XRD patterns of the pristine Cu powders and the EDA/NaOH treated Cu powders isolated from (d), respectively. The diffraction patterns at the top and bottom are the literature references for cubic Cu crystals (JCPDS 04-0836, black lines), cubic Cu_2O crystals (JCPDS 05-0667, blue lines), and CuO crystals (JCPDS 44-0706, orange lines), respectively. (c, d) Photos of the flask containing a mixture of Cu powders, EDA, and NaOH (c) before and (d) after stirring at room temperature for 1 hour, respectively. The flask contains 45 mg of Cu powders, 1.5 mL of EDA, and an aqueous solution (20 mL) of NaOH (15 M). (e) Photo of the supernatant isolated from (d).

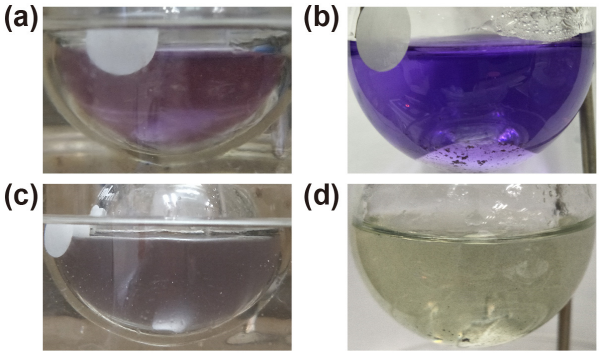

Fig. S15 (a, b) Photos of the flask containing a mixture of Cu powders and EDA (a) before and (b) after heating at 80 ºC for 1 hour without stirring, respectively. The flask contains 6.4 mg of Cu powders, 100 μL of EDA, and 21 mL of H_2O. (c, d) Photos of the flask containing a mixture of Cu powders, EDA and NaOH (c) before and (d) after heating at 80 ºC for 1 hour without stirring, respectively. The flask contains 6.4 mg of Cu powders, 100 μL of EDA, an aqueous solution (20 mL) of NaOH (15 M), and 1 mL of H_2O. Note that the Cu powders were dispersed in the mixture by stirring before heating.

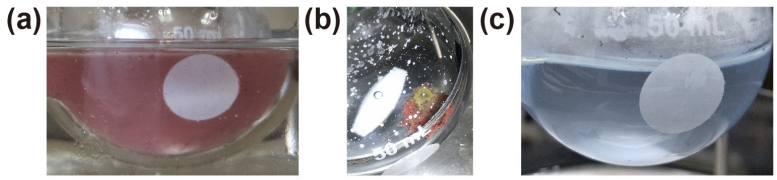

Fig. S16 (a) Photo of the flask containing a mixture of smooth Cu nanowires, EDA (100 μL) and an aqueous solution (20 mL) of NaOH (15 mL) before any treatment. (b) Corresponding photo of the mixture after heating at 80 ºC for 1 hour under stirring (200 rpm). After the treatment, no obvious color change was observed, and Cu nanowires became a large aggregate. (c) Corresponding photo of the mixture after another addition of EDA (300 μL) to the mixture shown in (b) and subsequent heating at 80 ºC for another 1 hour under stirring (200 rpm). Note that the smooth Cu nanowires were obtained according to the typical procedure described in experimental section, and the obtained Cu nanowires were dispersed in H_2O (1 mL) for this experiment.

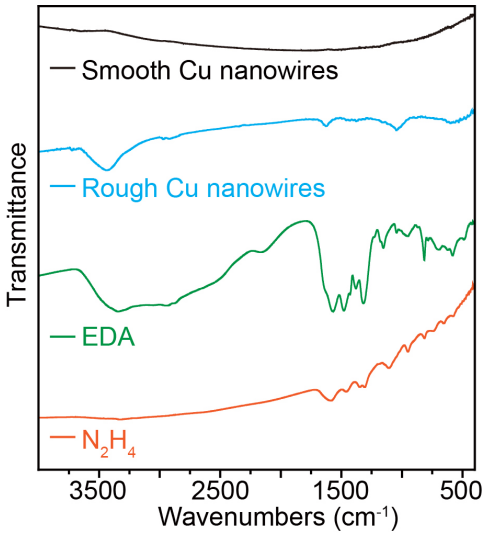

Fig. S17 FTIR spectra of smooth Cu nanowires, rough Cu nanowires, EDA and N_2H_4, respectively.

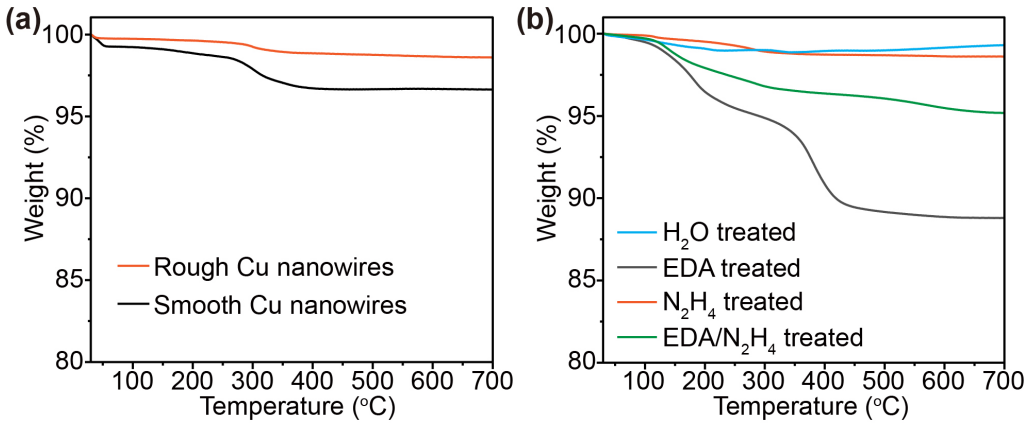

Fig. S18 (a) Thermogravimetric analysis curves of both smooth and rough Cu nanowires. The Cu nanowires were washed with water and dried under vacuum before the analysis. (b) Thermogravimetric analysis curves of Cu powders after different treatments. To prepare the samples of Cu powders, a mixture of Cu powders (15 mg) and a certain solution was first sonicated for 5 minutes. The Cu powders were then separated by centrifugation and dried under vacuum for further thermogravimetric analysis. The solutions for H_2O, EDA, N_2H_4, EDA/N_2H_4 treatments are H_2O (750 μL), EDA (500 μL), N_2H_4 (150 μL), and a mixture of EDA (500 μL) and N_2H_4 (150 μL), respectively.

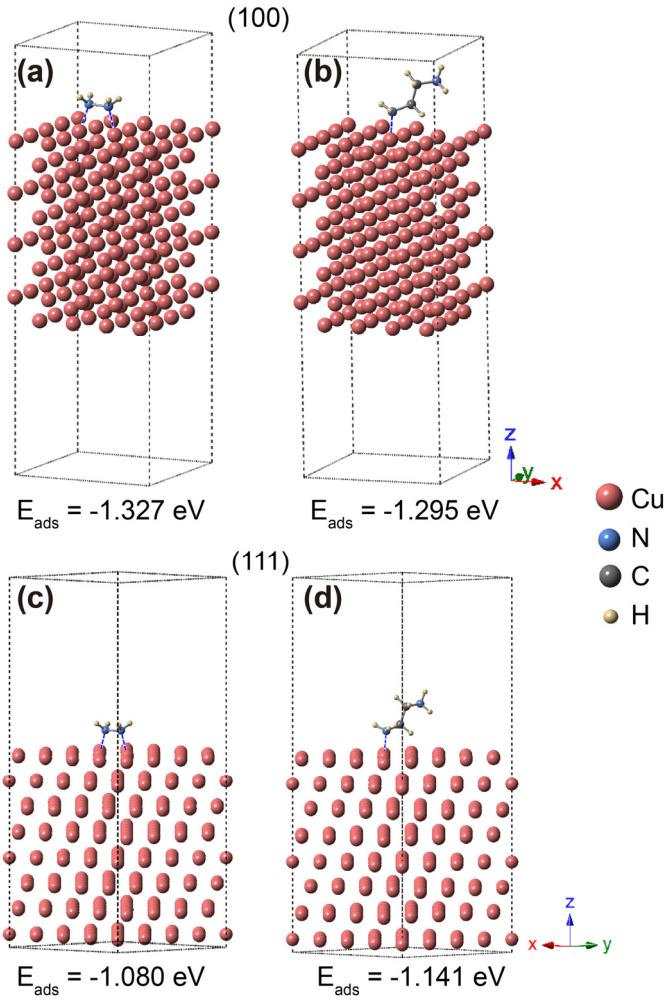

Fig. S19 Optimized surface configurations for adsorption of hydrazine (a, c) and ethylenediamine (b, d) on the Cu (100) (top panel) and (111) (bottom panel) surfaces. The calculated adsorption energies (E_{ads}) are also given.

All the first-principle calculations were performed based on the Density Functional Theory (DFT), using the Vienna Ab initio Simulation Package (VASP) code.[1-3] The exchange correlation potential was described using the Perdew, Burke and Ernzerhof (PBE) functional within the generalized gradient approximation (GGA).[4] The energy convergence for the relaxation was chosen to be less than 10^{-5} eV/Å. Taking into account nonlocal van der Waals interaction, we adopted the newly developed vdW density functional (optB86b-vdW) in our study.[5] To simulate the surface models, we adopted two 3×3 supercells for (001) and (111) surfaces and each model consists of eight copper slab layers. A ~25 Å vacuum layer along the z-axis is added to avoid the mirror interactions between the neighboring images. The Brillouin zone was sampled by a 3×3×1 k-point mesh using Monkhorst-Pack (MP) method. For the hydrazine on copper surfaces, we considered the lowest-energy eclipsed N_2H_4 configuration, similar

to the previous report.[6] For ethylenediamine adsorption, the amine group forms a single bond with one Cu atom on the surface.[7] The adsorption energy was calculated by the following equation:

$$E_{ads} = E_{surface+molecule} - E_{surface} - E_{molecule}$$

where $E_{surface+molecule}$, $E_{surface}$, and $E_{molecule}$ are the total energy of the optimized system, the total energy of bare surface, and the total energy of isolated molecule, respectively.

References:

1. G. Kresse and J. Hafner, *Phys. Rev. B*, 1993, **47**, 558.
2. G. Kresse and J. Furthmüller, *Comput. Mat. Sci.*, 1996, **6**, 15.
3. G. Kresse and J. Furthmüller, *Phys. Rev. B*, 1996, **54**, 11169.
4. J. P. Perdew, J. A. Chevary, S. H. Vosko, K. A. Jackson, M. R. Pederson, D. J. Singh, and C. Fiolhais, *Phys. Rev. B*, 1992, **46**, 6671.
5. T. Thonhauser, V. R. Cooper, S. Li, A. Puzder, P. Hyldgaard, and D. C. Langreth, *Phys. Rev. B*, 2007, **76**, 125112.
6. S. S. Tafreshi, A. Roldan, and N. H. de Leeuw, *J. Phys. Chem. C*, 2014, **118**, 26103.
7. J. Koo, S. Kwon, N. R. Kim, K. Shin, and H. M. Lee, *J. Phys. Chem. C*, 2016, **120**, 3334.

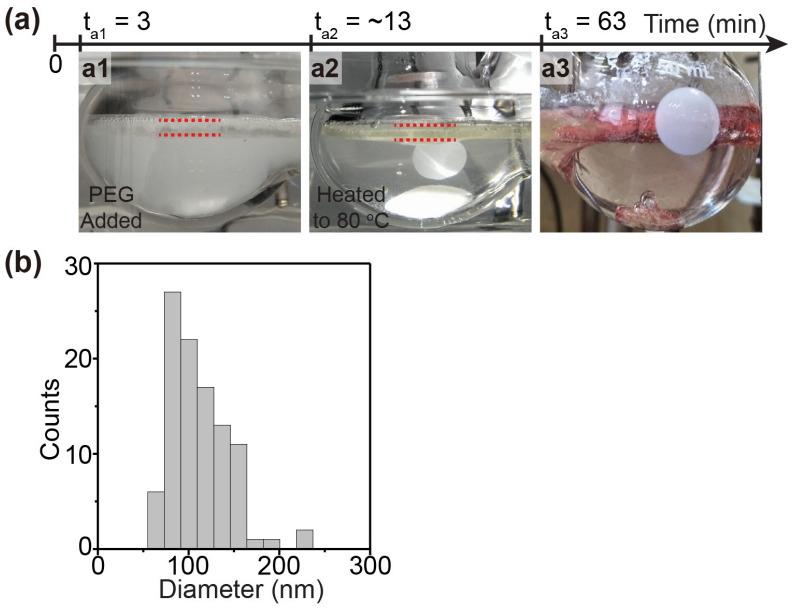

Fig. S20 (a) Recorded synthetic process of Cu nanowires in the presence of an upper layer of polyethylene glycol. (a1-a3): photos of the reaction mixture (a1) after the addition of polyethylene glycol, (a2) after heated to 80 °C, and (a3) after the reaction, respectively. Note that the timeline on top illustrates the progress of the reaction, and the beginning of the reaction (t = 0 min) is denoted as the time point when $Cu(NO_3)_2$ is added to the reaction system. The red dotted lines in (a1) and (a2) indicate the upper layer of polyethylene glycol. (b) Corresponding diameter distribution of the as-synthesized Cu nanowires shown in Fig. 5b.

The experimental procedure used here was mostly the same as that for synthesizing rough Cu nanowires, and the main difference lay in the addition of polyethylene glycol. In a typical experiment, $Cu(NO_3)_2$ (0.1 M, 1 mL), EDA (400 μL), and N_2H_4 (20 μL) were added sequentially, with an time interval of 30 seconds, to a flask containing an aqueous solution of NaOH (20 mL, 15 M) under intense stirring. The resulting mixture was then stirred intensely for 2 minutes, yielding a well-mixed reaction mixture. Subsequently, the mixture was stirred continuously at 200 rpm, 5 mL of polyethylene glycol was added, and the resulting mixture was then heated to 80 °C within ~10 minutes. After the reaction continued for ~50 minutes under steady stirring, the mixture was naturally cooled to room temperature. The as-prepared Cu nanowires were separated by centrifugation, thoroughly washed three times with an aqueous solution containing N_2H_4 (3 wt%), and finally stored in an aqueous solution (4 mL) containing N_2H_4 (3 wt%) for further use.

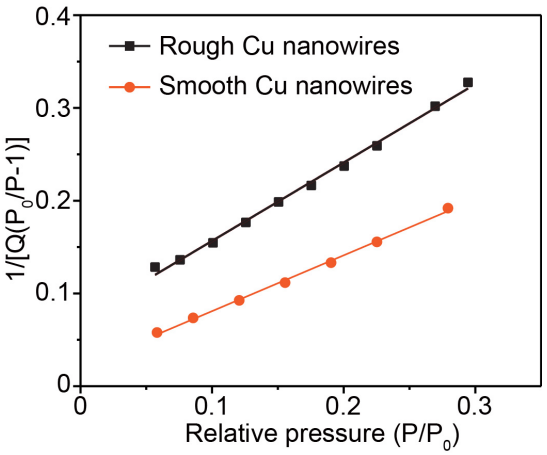

Fig. S21 BET surface area plots of both smooth and rough Cu nanowires.

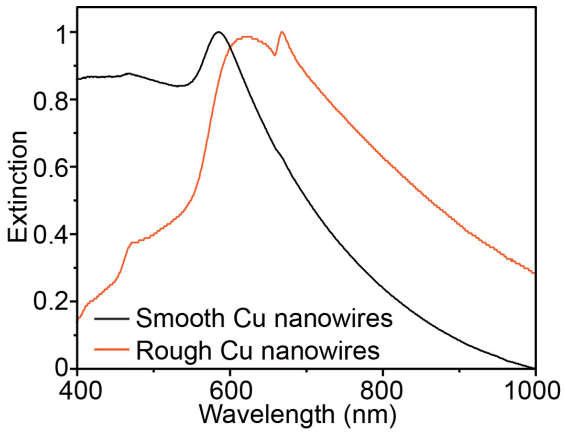

Fig. S22 Normalized visible-near infrared extinction spectra for both smooth and rough Cu nanowires.

Table S1. Electrocatalytic performance of Cu nanowires in CO_2 reduction.

Potential	Smooth Cu nanowire		Rough Cu nanowire	
(vs. Ag/AgCl (3 M KCl))	FE_{CO} %[a]	FE_{HCOOH} %[a]	FE_{CO} %[a]	FE_{HCOOH} %[a]
-1.3 V	6.6	33.6	2.8	47.2
-1.5 V	5.6	40.7	4.5	56.3
-1.8 V	2.6	32.3	3.7	46.3

[a]FE: faradaic efficiency.

The bulk electrolysis for 1 hour was carried out in a gas tight reactor using the carbon plate (1×1 cm^2) spin coated with Cu nanowires (loading of ~0.9 mg/cm^2) as the working electrode. The electrolyte was 0.1 M $KHCO_3$ (60 mL), the reference electrode was Ag/AgCl (3 M KCl), and the counter electrode was Pt mesh. Prior to electrolysis, the reactor was purged with CO_2 for 30 minutes to ensure CO_2 atmosphere. During electrolysis, a constant potential (-1.3, -1.5 or -1.8 V) was applied on the working electrode, and the current was monitored and recorded. After the electrolysis, the gaseous product was analyzed by a gas chromatograph (Shimadzu, GC-2014), while the liquid product was analyzed by a liquid chromatograph (Hitachi, Primaide). In this study, CO and HCOOH were the main reduction products. The faradaic efficiency (FE) was calculated by dividing the electrons needed for reduction product (CO or HCOOH) by the electrons passing through working electrode-counter electrode circuit, which can be described by the following equation:

$$FE = nzF/Q$$

where n is the molar amount of a product (in the unit of mol); z is the number of electrons consumed to produce one product molecule (z = 2, for the product of CO or HCOOH); F is the Faraday constant (F = 96500 C/mol); Q is the amount of electrons consumed during electrolysis, and can be calculated by integrating electrolytic current against time (in the unit of C).

Particularly, the CO product was maintained at relative low levels for both kinds of nanowires, and rough Cu nanowires presented improved selectivity (~40% improvement in faradaic efficiency) towards formic acid, a value-added product, than

that catalysed by smooth Cu nanowires. These findings show that morphology manipulation of Cu nanowires can adjust their catalytic performance.